Joint 48th IEEE Conference on Decision and Control and
28th Chinese Control Conference
Shanghai, P.R. China, December 16-18, 2009

Hybrid Control Strategy for Five-Fingered Smart Prosthetic Hand

Cheng-Hung Chen, *Student Member, IEEE*, D. Subbaram Naidu, *Fellow, IEEE*, Alba Perez-Gracia, and Marco P. Schoen, *Member, IEEE*

Abstract—**This paper presents a hybrid of soft computing or control technique of adaptive neuro-fuzzy inference system (ANFIS) and hard computing or control technique of finite-time linear quadratic optimal control for the 14 degrees of freedom (DOFs), five-fingered smart prosthetic hand. In particular, ANFIS is used for inverse kinematics, and the optimal control is used for feedback linearized dynamics to minimize tracking error. The simulations of this hybrid controller, when compared with the proportional-integral-derivative (PID) controller showed enhanced performance.**

Index Terms—**Prosthetic Hand, Optimal Control, PID Control, Adaptive Neuro-Fuzzy Inference System, Hybrid Control**

I. Introduction

Over the last several yeas, attempts have been made to build a prosthetic hand to replace human hand that fully simulate the various natural/human-like operations of moving, grasping, lifting, twisting and so on. Replicating the human hand in all its various functions is still a challenging task due to the extreme complexity of human hand, which has 27 bones, controlled by about 38 muscles to provide the hand with 22 degrees of freedom (DOFs), and incorporates about 17,000 tactile units of 4 different units [1]. Artificial hands have been around for the last several years developed by various researchers in the field [1]–[4]. However, about 35% of the amputees [5] do not use their prosthetic hand regularly due to various reasons such as poor functionality of the presently available prosthetic hands and psychological problems. To overcome these problems, one has to design and develop an artificial hand which "mimics the human hand as closely as possible," both in functionality and appearance.

Soft computing/control (SC) or computational intelligence (CI) [6] is an emerging field based on synergy and seamless integration of neural networks (NN), fuzzy logic (FL) and genetic algorithms (GA) [7]. Arslan et al. [8] developed the biomechanical model with a tendon configuration of the 3 DOFs index finger of the human hand and the fuzzy sliding mode controller in which a fuzzy logic unit tuned the slope of the sliding surface was introduced to generate the required tendon forces during closing and opening motion. Onozato and Maeda [9] utilized two neural networks learning inverse kinematic and inverse dynamic to control the positions of 2 DOFs SCARA robot. Aggarwal et al. [10] obtained the neural recordings from rhesus monkeys with three different movements, the flexion/extension of each finger, the rotation of wrist and dexterous grasps and designed separate decoding filters for each movement by using multilayer feedforward artificial neural network (ANN) in order to be implemented in real-time MATLAB/Simulink. An online decentralized neural network control design without deriving the dynamic model for a class of large-scale uncertain robot manipulator systems was proposed by Tan et al. [11]. Kato et al. [12] expressed the reaction of brains to the adaptable prosthetic system for a 13 DOFs EMG signal controlled prosthetic hand with an EMG pattern recognition learning by artificial neural networks. In addition, functional magnetic resonance imaging (f-MRI) was used to analyze the reciprocal adaptation between the human brain and the prosthetic hand by the plasticity of the motor and sensory cortex area in brains based on the variations in the phantom upper limb. Marcos et al. [13] proposed the closed-loop pseudo-inverse method with genetic algorithms (CLGA) to minimize the largest joint displacement between two adjacent configurations, the total level of joint velocities, the joint accelerations, the total joint torque, and the total joint power consumption for the trajectory planning of 3 DOFs redundant robots. Kamikawa and Maeno [14] used genetic algorithm to optimize locations of pivots and grasping force and designed one ultrasonic motor to move 15 compliant joints for an underactuated five-finger prosthetic hand.

Hard computing/control (HC) techniques comprise proportional integral derivative (PID) control [15]–[18], optimal control [19], [20] and so on with specific applications to prosthetics. SC can be used at upper levels of the overall mission where human involvement and decision making is of primary importance. HC can be used at lower levels for accuracy, precision, stability and robustness. Therefore, the integration of SC and HC methodologies could solve problems that cannot be solved satisfactorily by using either methodology alone and lead to high performance, robust, autonomous and cost-effective systems.

Our previous works [17], [18] for a two-fingered (thumb and index finger) smart prosthetic hand showed that PID controller results in the overshooting and oscillation, which were

Cheng-Hung Chen is with the Measurement and Control Engineering Research Center and the Department of Biological Sciences, Idaho State University, ID 83209, USA (email: chenchen@isu.edu).

D. Subbaram Naidu is with the Measurement and Control Engineering Research Center and the Department of Electrical Engineering, Idaho State University, ID 83209, USA (email: naiduds@isu.edu).

Alba Perez-Gracia is with the Measurement and Control Engineering Research Center and the Department of Mechanical Engineering, Idaho State University, ID 83209, USA on leave with Institut de Robotica i Informatica Industrial (UPC-CSIC) c/ Llorens i Artigas 4-6, Barcelona, Spain (email: perealba@isu.edu).

Marco P. Schoen is with the Measurement and Control Engineering Research Center and the Department of Mechanical Engineering, Idaho State University, ID 83209, USA (email: schomarc@isu.edu).

978-1-4244-3872-3/09/$25.00 ©2009 IEEE

also demonstrated by Subudhi and Morris [15] and Liu et al. [16]. To overcome the problem, fusion of soft computing technique of adaptive neuro-fuzzy inference system (ANFIS) and finite-time linear quadratic optimal control strategy for 14 DOFs prosthetic hand is precisely the main goal of this work.

In this paper, we first consider briefly the trajectory planning problem, human hand anatomy and the inverse kinematics for two-link thumb and the remaining three-link fingers (index, middle, ring, and little) using ANFIS. Next, the dynamics of the hand is derived and feedback linearization technique is used to obtain *linear* tracking error dynamics. Then the finite-time linear quadratic optimal controller is designed to minimize the tracking error. The resulting overall hybrid system incorporating both soft and hard control techniques is simulated with practical data for the hand and found to be better than the previous works. The last section provides conclusions and future work.

II. Modeling

A. Trajectory Planning and Inverse Kinematics

The trajectory planning using cubic polynomial was discussed in our previous work [17], [18], [21]–[23] for a two-fingered (thumb and index finger) smart prosthetic hand. As shown in Figure 1, index finger, middle finer, ring finer, and

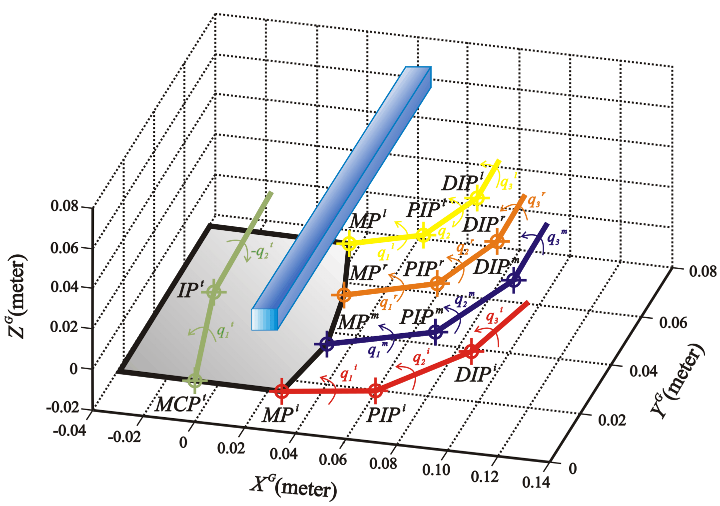

Fig. 1. The Joints of Five-Finger Prosthetic Hand Reaching a Rectangular Rod

little finger include three revolute joints in order to do the angular movements. Metacarpal-phalangeal (MCP) joint is located between metacarpal and proximal phalange bone; proximal and distal interphalangeal (PIP and DIP) joints separate the phalangeal bones. Thumb contains metacarpal-phalangeal (MCP) and interphalangeal (IP) joints [24]. In this work, q_1^j, q_2^j and q_3^j represent the angular positions (or joint angles) of the first joint MCP^j, the second joint PIP^j and the third joint DIP^j of index finger ($j = i$), middle finger ($j = m$), ring finger ($j = r$) and little finger ($j = l$), respectively; q_1^t and q_2^t are the angular positions of the first joint MCP^t and the second joint IP^t of thumb (t).

A desired trajectory is usually specified in *Cartesian* space and the trajectory controller is easily performed in the *joint* space. Hence, it is necessary to convert Cartesian trajectory planning to the joint space [25]–[27]. Using inverse kinematics, the joint angles of each finger need to be obtained from the known fingertip positions (*joint space*). Then the angular velocities and angular accelerations of each finger can be obtained from the velocities and accelerations of fingertips by Jocobian. Figure 2 shows that X^G, Y^G, and

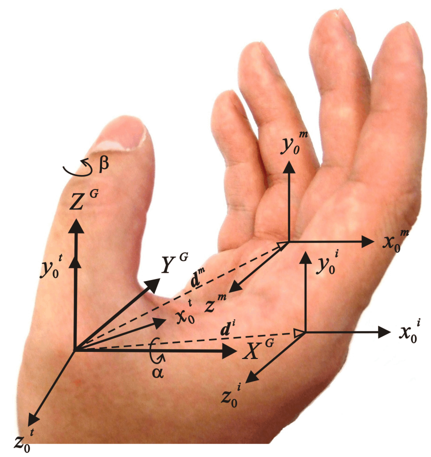

Fig. 2. The Definition of Global Coordinate and Local Coordinates

Z^G are the three axes of the global coordinate. The local coordinate x^t-y^t-z^t of the thumb can be reached by rotating through angles α and β to X^G and Y^G of the global coordinate, subsequently. The local coordinate x^i-y^i-z^i of index finger can be obtained by rotating through angle α to X^G and then translating the vector $\mathbf{d^i}$ of the global coordinate; similarly, the local coordinate x^j-y^j-z^j of middle finger ($j = m$), ring finger ($j = r$), and little finger ($j = l$) can be obtained by rotating through angle α to X^G and then translating the vector $\mathbf{d^j}$ ($j = m$, r and l) of the global coordinate. The inverse kinematics of two-link thumb and three-link fingers was discussed in our previous publications [17], [18], [21]–[23] for a two-fingered (thumb and index finger) smart prosthetic hand.

B. Dynamics of Hand

The dynamic equations of hand motion are derived via Lagrangian approach using kinetic energy and potential energy as [25]–[28]

$$\frac{d}{dt}\left(\frac{\partial \mathcal{L}}{\partial \dot{\mathbf{q}}}\right) - \frac{\partial \mathcal{L}}{\partial \mathbf{q}} = \boldsymbol{\tau}, \tag{1}$$

where $\mathcal{L}$ is Lagrangian; $\dot{\mathbf{q}}$ and $\mathbf{q}$ represent the angular velocity and angle vectors of joints, respectively; $\boldsymbol{\tau}$ is the given torque vector at joints. The Lagrangian $\mathcal{L}$ can be expressed as

$$\mathcal{L} = T - V, \tag{2}$$

where T and V denote kinetic and potential energies, respectively. Substituting (2) into (1) gives the relation as

$$\mathbf{M}(\mathbf{q})\ddot{\mathbf{q}} + \mathbf{C}(\mathbf{q}, \dot{\mathbf{q}}) + \mathbf{G}(\mathbf{q}) = \boldsymbol{\tau}, \tag{3}$$

where $\mathbf{M}(\mathbf{q})$ is the inertia matrix; $\mathbf{C}(\mathbf{q},\dot{\mathbf{q}})$ is the Coriolis/centripetal vector and $\mathbf{G}(\mathbf{q})$ is the gravity vector. (3) can be also written as

$$\mathbf{M}(\mathbf{q})\ddot{\mathbf{q}} + \mathbf{N}(\mathbf{q},\dot{\mathbf{q}}) = \boldsymbol{\tau}, \tag{4}$$

where $\mathbf{N}(\mathbf{q},\dot{\mathbf{q}})$ = $\mathbf{C}(\mathbf{q},\dot{\mathbf{q}})$+$\mathbf{G}(\mathbf{q})$ represents nonlinear terms. The dynamic relations for the two-link thumb and the three-link fingers are quite lengthy and omitted here due to lack of space [8], [21], [29].

III. Control Techniques

A. Feedback Linearization

The nonlinear dynamics represented by (4) is to be converted into a linear state-variable system by finding a transformation using feedback linearization technique [28], [30]. Alternative state-space equations of the dynamics can be obtained by defining the position/velocity state $\mathbf{x}(t)$ of the joints as

$$\mathbf{x}(t) = \left[\mathbf{q}(t)' \quad \dot{\mathbf{q}}(t)'\right]'. \tag{5}$$

Let us repeat the dynamical model and rewrite (4) as

$$\frac{d}{dt}\dot{\mathbf{q}}(t) = -\mathbf{M}(\mathbf{q}(t))^{-1}\left[\mathbf{N}(\mathbf{q}(t),\dot{\mathbf{q}}(t)) - \boldsymbol{\tau}(t)\right]. \tag{6}$$

Thus, from (5) and (6), we can derive a linear state-variable equation in *Brunovsky canonical form* as

$$\dot{\mathbf{x}}(t) = \begin{bmatrix} \mathbf{0} & \mathbf{I} \\ \mathbf{0} & \mathbf{0} \end{bmatrix}\mathbf{x}(t) + \begin{bmatrix} \mathbf{0} \\ \mathbf{I} \end{bmatrix}\mathbf{u}(t) \tag{7}$$

with its control input vector given by

$$\mathbf{u}(t) = -\mathbf{M}(\mathbf{q}(t))^{-1}\left[\mathbf{N}(\mathbf{q}(t),\dot{\mathbf{q}}(t)) - \boldsymbol{\tau}(t)\right]. \tag{8}$$

Let us suppose the prosthetic hand is required to track the desired trajectory $\mathbf{q}_d(t)$ described under path generation or tracking. Then, the tracking error $\mathbf{e}(t)$ is defined as

$$\mathbf{e}(t) = \mathbf{q}_d(t) - \mathbf{q}(t). \tag{9}$$

Here, $\mathbf{q}_d(t)$ is the *desired* angle vector of joints and can be obtained by trajectory planning [17], [18], [21]–[23]; $\mathbf{q}(t)$ is the *actual* angle vector of joints. Differentiating (9) twice, to get

$$\dot{\mathbf{e}}(t) = \dot{\mathbf{q}}_d(t) - \dot{\mathbf{q}}(t), \quad \ddot{\mathbf{e}}(t) = \ddot{\mathbf{q}}_d(t) - \ddot{\mathbf{q}}(t). \tag{10}$$

Substituting (6) into (10) yields

$$\ddot{\mathbf{e}}(t) = \ddot{\mathbf{q}}_d(t) + \mathbf{M}(\mathbf{q}(t))^{-1}\left[\mathbf{N}(\mathbf{q}(t),\dot{\mathbf{q}}(t)) - \boldsymbol{\tau}(t)\right] \tag{11}$$

from which the control function can be defined as

$$\mathbf{u}(t) = \ddot{\mathbf{q}}_d(t) + \mathbf{M}(\mathbf{q}(t))^{-1}\left[\mathbf{N}(\mathbf{q}(t),\dot{\mathbf{q}}(t)) - \boldsymbol{\tau}(t)\right]. \tag{12}$$

This is often called the *feedback linearization* control law, which can also be inverted to express it as

$$\boldsymbol{\tau}(t) = \mathbf{M}(\mathbf{q}(t))\left[\ddot{\mathbf{q}}_\mathbf{d}(t) - \mathbf{u}(t)\right) + \mathbf{N}(\mathbf{q}(t),\dot{\mathbf{q}}(t)]. \tag{13}$$

Using the relations (10) and (12), and defining state vector $\mathbf{x}(t) = [\mathbf{e}(t)' \quad \dot{\mathbf{e}}(t)']'$, the *tracking error dynamics* can be written as

$$\dot{\mathbf{x}}(t) = \begin{bmatrix} \mathbf{0} & \mathbf{I} \\ \mathbf{0} & \mathbf{0} \end{bmatrix}\mathbf{x}(t) + \begin{bmatrix} \mathbf{0} \\ \mathbf{I} \end{bmatrix}\mathbf{u}(t). \tag{14}$$

Note that this is in the form of a *linear* system such as

$$\dot{\mathbf{x}}(t) = \mathbf{A}\mathbf{x}(t) + \mathbf{B}\mathbf{u}(t). \tag{15}$$

B. Hybrid PID Controller

Figure 3 shows the block diagram of a hybrid PID controller for five-fingered prosthetic hand with control signal as

$$\mathbf{u}(t) = -\mathbf{K_P}\mathbf{e}(t) - \mathbf{K_I}\int \mathbf{e}(t)dt - \mathbf{K_D}\dot{\mathbf{e}}(t) \tag{16}$$

with the proportional $\mathbf{K_P}$, integral gain matrix $\mathbf{K_I}$, and derivative $\mathbf{K_D}$ diagonal gain matrices. We then rewrite (13) as

$$\begin{aligned} \boldsymbol{\tau}(t) \;=\;& \mathbf{M}(\mathbf{q}(t))[\ddot{\mathbf{q}}_\mathbf{d}(t) + \mathbf{K_P}\mathbf{e}(t) + \mathbf{K_I}\int \mathbf{e}(t)dt \\ & + \mathbf{K_D}\dot{\mathbf{e}}(t)) + \mathbf{N}(\mathbf{q}(t),\dot{\mathbf{q}}(t)]. \end{aligned} \tag{17}$$

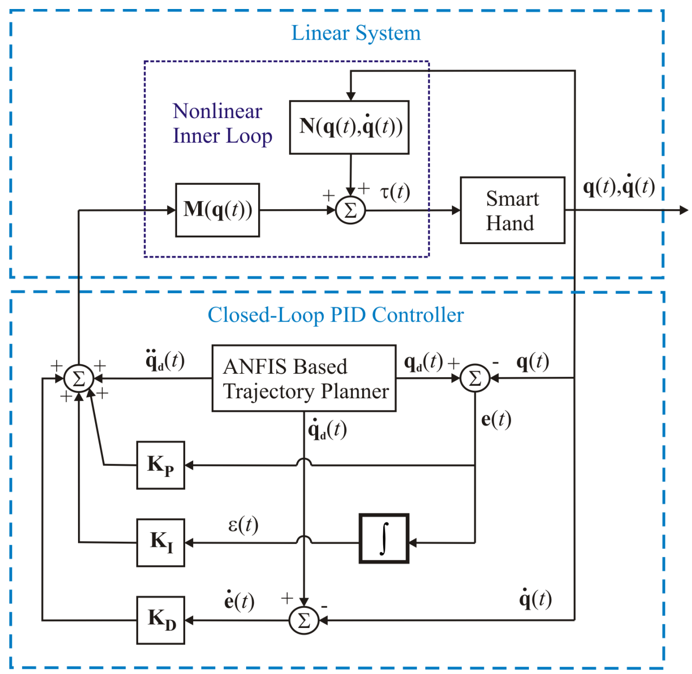

Fig. 3. Block Diagram of a Hybrid PID Controller for Prosthetic Hand

C. Hybrid Finite-Time Linear Quadratic Optimal Control

For the linear system (15), we can formulate the finite-time linear quadratic optimal control problem (as shown in Figure 4) by defining a performance index J [20] such as

$$\begin{aligned} J \;=\;& \frac{1}{2}\mathbf{x}'(t_f)\mathbf{F}(t_f)\mathbf{x}(t_f) \\ & + \frac{1}{2}\int_{t_0}^{t_f}\left[\mathbf{x}'(t)\mathbf{Q}(t)\mathbf{x}(t) + \mathbf{u}'(t)\mathbf{R}(t)\mathbf{u}(t)\right]dt \end{aligned} \tag{18}$$

where the terminal cost matrix $\mathbf{F}(t_f)$ and the error weighted matrix $\mathbf{Q}(t)$ are positive $semidefinite$ matrices, respectively; the control weighted matrix $\mathbf{R}(t)$ is a positive $definite$ matrix. The optimal control $\mathbf{u}^*(t)$ is given by

$$\mathbf{u}^*(t) = -\mathbf{R}^{-1}(t)\mathbf{B}'\mathbf{P}(t)\mathbf{x}^*(t) = -\mathbf{K}(t)\mathbf{x}^*(t). \tag{19}$$

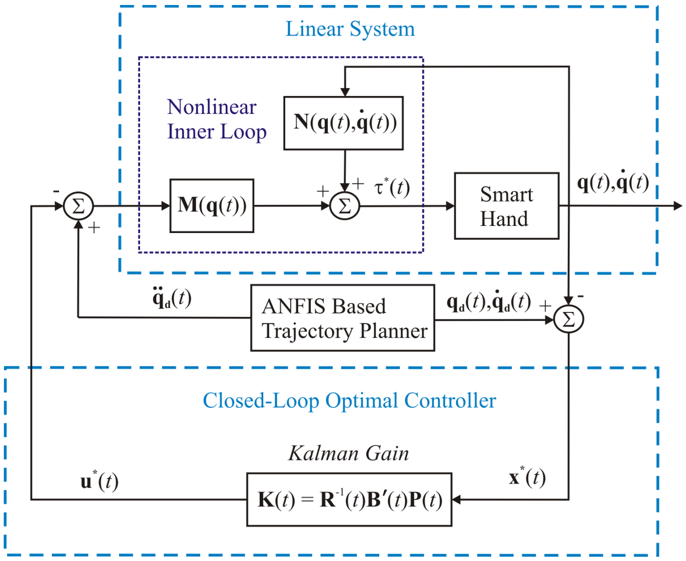

Fig. 4. Block Diagram of Hybrid Optimal Controller for Prosthetic Hand

Here, $\mathbf{K}(t) = \mathbf{R}^{-1}(t)\mathbf{B}'\mathbf{P}(t)$ is called *Kalman gain* and $\mathbf{P}(t)$, the symmetric *positive definite* matrix (for all $t \in [t_0, t_f]$), is the solution of the matrix differential Riccati equation (DRE)

$$\dot{\mathbf{P}}(t) = -\mathbf{P}(t)\mathbf{A} - \mathbf{A}'\mathbf{P}(t) - \mathbf{Q}(t) + \mathbf{P}(t)\mathbf{B}\mathbf{R}^{-1}(t)\mathbf{B}'\mathbf{P}(t) \quad (20)$$

satisfying the *final* condition

$$\mathbf{P}(t = t_f) = \mathbf{F}(t_f). \quad (21)$$

The optimal state $\mathbf{x}^*$ is the solution of

$$\dot{\mathbf{x}}^*(t) = \left[\mathbf{A} - \mathbf{B}\mathbf{R}^{-1}(t)\mathbf{B}'\mathbf{P}(t)\right]\mathbf{x}^*(t). \quad (22)$$

Therefore, the required torque $\boldsymbol{\tau}^*(t)$ can be calculated by the optimal control $\mathbf{u}^*(t)$.

$$\boldsymbol{\tau}^*(t) = \mathbf{M}(\mathbf{q}(t))\left[\ddot{\mathbf{q}}_d(t) - \mathbf{u}^*(t)\right) + \mathbf{N}(\mathbf{q}(t), \dot{\mathbf{q}}(t)]. \quad (23)$$

We also intend to use infinite-time optimal regulator to avoid backward integration of the DRE, especially for on-line (real-time) design and implementation.

IV. Simulation Results and Discussion

When thumb and the other four fingers are doing extension/flexion movements, the workspace of fingertips is restricted to the maximum angles of joints. Referring to inverse kinematics, Figure 5 explains that the workspace of the thumb fingertip, in which the first and second joint angles are constrained in the ranges of [0,90] and [-80,0] (degrees). The first, second, and third joint angles of the other four fingers are constrained in the ranges of [0,90], [0,110] and [0,80] (degrees), respectively [31]. Thus, the green, red, blue, orange, and yellow regions respectively show the reachable fingertip positions of thumb and the other four fingers. Note that the X^G axis is of different scale to show more clearly the individual three-dimensional regions of reach.

Next, we present simulations with a PID controller and a finite-time linear quadratic optimal controller for the 14 DOFs five-fingered smart prosthetic hand.

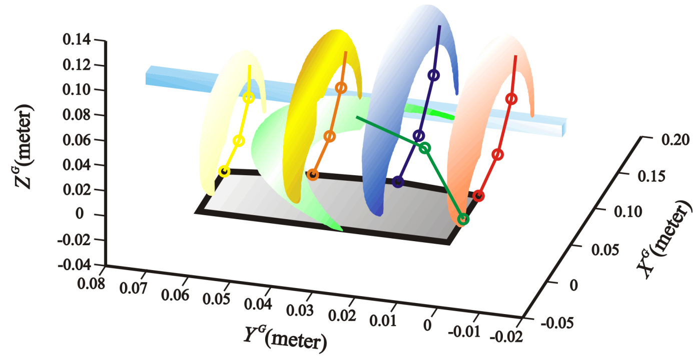

Fig. 5. Workspace of the Five-Fingered Prosthetic Hand with a Rectangular Rod

A. Hybrid PID Controller

The parameters of the two-link thumb/three-link index finger [32] were related to desired trajectory. All parameters of the smart prosthetic hand selected for the simulations are given in Table I and the side length and length of the target rectangular rod are 0.010 and 0.100 (m), respectively. The relating parameters between the global coordinate and the local coordinates are defined in Table II. In addition, all links are assumed as circular cylinder with the radius (R) 0.010 (m), so the inertia I^j_{zzk} of each link k of each finger j (j = t, i, m, r, and l) can be calculated as

$$I^j_{zzk} = \frac{1}{4}m^j_k R^2 + \frac{1}{3}m^j_k {L^j_k}^2. \quad (24)$$

All initial actual angles are zero and all PID diagonal coefficients, $\mathbf{K_P}$, $\mathbf{K_I}$ and $\mathbf{K_D}$, are 100.

B. Hybrid Optimal Controller

As for optimal control coefficients, $\mathbf{A}$, $\mathbf{B}$, $\mathbf{F}(t_f)$, $\mathbf{R}(t)$ and $\mathbf{Q}(t)$ of all fingers are chosen as

$$\mathbf{A} = \begin{bmatrix} \mathbf{0} & \mathbf{I} \\ \mathbf{0} & \mathbf{0} \end{bmatrix}, \quad \mathbf{B} = \begin{bmatrix} \mathbf{0} \\ \mathbf{I} \end{bmatrix}, \quad \mathbf{F}(t_f) = \mathbf{0}, \quad \mathbf{R}(t) = \frac{1}{30}\mathbf{I},$$

$$\mathbf{Q}(t)^t = \begin{bmatrix} \mathbf{Q_{11}} & \mathbf{Q_{12}} \\ \mathbf{Q_{12}} & \mathbf{Q_{22}} \end{bmatrix}, \quad \mathbf{Q}(t)^j = \begin{bmatrix} \mathbf{Q_{11}} & \mathbf{Q_{12}} & \mathbf{Q_{13}} \\ \mathbf{Q_{12}} & \mathbf{Q_{22}} & \mathbf{Q_{23}} \\ \mathbf{Q_{13}} & \mathbf{Q_{23}} & \mathbf{Q_{33}} \end{bmatrix},$$

$$\mathbf{Q_{11}} = \begin{bmatrix} 10 & 2 \\ 2 & 10 \end{bmatrix}, \quad \mathbf{Q_{22}} = \begin{bmatrix} 30 & 0 \\ 0 & 30 \end{bmatrix}, \quad \mathbf{Q_{33}} = \begin{bmatrix} 20 & 1 \\ 1 & 20 \end{bmatrix},$$

$$\mathbf{Q_{12}} = \begin{bmatrix} -4 & 4 \\ 3 & -6 \end{bmatrix}, \mathbf{Q_{13}} = \begin{bmatrix} -4 & 4 \\ 3 & -6 \end{bmatrix}, \mathbf{Q_{23}} = \begin{bmatrix} -4 & 3 \\ 4 & -6 \end{bmatrix}.$$

Here j = i, m, r, and l.

Figures 6 to 10 show the simulations with hybrid PID controller and hybrid optimal controller. It is clearly seen the superiority of the hybrid optimal controller in suppressing the overshoots and transients associated with the hybrid PID controller.

V. Conclusions and Future Work

This paper focussed on hybrid of soft computing or control technique of adaptive neuro-fuzzy inference system (ANFIS) and hard computing or control technique of finite-time linear quadratic optimal control for the 14 DOFs, five-fingered smart prosthetic hand. The ANFIS is a fuzzy inference system which is implemented in the framework

TABLE I

PARAMETER SELECTION OF THE SMART HAND

Parameters	Values
Thumb	
Time $(t_0,t_f)^*$	0, 20 (sec)
Desired Initial Position $(X_0^t,Y_0^t)^{**}$	0.035, 0.060 (m)
Desired Final Position $(X_f^t,Y_f^t)^{**}$	0.0495, 0.060 (m)
Desired Initial Velocity $(\dot{X}_0^t,\dot{Y}_0^t)^*$	0, 0 (m/s)
Desired Final Velocity $(\dot{X}_f^t,\dot{Y}_f^t)^*$	0, 0 (m/s)
Length (L_1^t,L_2^t)	0.040, 0.040 (m)
Mass (m_1^t,m_2^t)	0.043, 0.031 (kg)
Index Finger	
Desired Initial Position $(X_0^i,Y_0^i)^{**}$	0.065, 0.080 (m)
Desired Final Position $(X_f^i,Y_f^i)^{**}$	0.010, 0.060 (m)
Length (L_1^i,L_2^i,L_3^i)	0.040, 0.040, 0.030 (m)
Mass (m_1^i,m_2^i,m_3^i)	0.045, 0.025, 0.017 (kg)
Middle Finger	
Desired Initial Position $(X_0^m,Y_0^m)^{**}$	0.065, 0.080 (m)
Desired Final Position $(X_f^m,Y_f^m)^{**}$	0.005, 0.060 (m)
Length (L_1^m,L_2^m,L_3^m)	0.044, 0.044, 0.033 (m)
Mass (m_1^m,m_2^m,m_3^m)	0.050, 0.028, 0.017 (kg)
Ring Finger	
Desired Initial Position $(X_0^r,Y_0^r)^{**}$	0.065, 0.080 (m)
Desired Final Position $(X_f^r,Y_f^r)^{**}$	0.010, 0.060 (m)
Length (L_1^r,L_2^r,L_3^r)	0.040, 0.040, 0.030 (m)
Mass (m_1^r,m_2^r,m_3^r)	0.041, 0.023, 0.014 (kg)
Little Finger	
Desired Initial Position $(X_0^l,Y_0^l)^{**}$	0.055, 0.080 (m)
Desired Final Position $(X_f^l,Y_f^l)^{**}$	0.020, 0.060 (m)
Length (L_1^l,L_2^l,L_3^l)	0.036, 0.036, 0.027 (m)
Mass (m_1^l,m_2^l,m_3^l)	0.041, 0.023, 0.014 (kg)

*All fingers use the same parameters.
**All parameters are in local coordinates.

TABLE II

PARAMETER SELECTION OF THE RELATION BETWEEN GLOBAL AND LOCAL COORDINATES

Parameters	Values
α	90 (degrees)
β	45 (degrees)
$\mathbf{d^i}$	(0.035, 0, 0) (m)
$\mathbf{d^m}$	(0.040, 0, -0.020) (m)
$\mathbf{d^r}$	(0.035, 0, -0.040) (m)
$\mathbf{d^l}$	(0.025, 0, -0.060) (m)

of adaptive networks which provides the best optimization tool to find parameters that best fits the data. In particular, ANFIS was used for inverse kinematics, and the optimal control was used to minimize tracking error using feedback linearized dynamics . The simulations of this hybrid controller, when compared with the proportional-integral-derivative (PID) controller showed enhanced performance. Work is underway to extend this methodology to 22 DOFs, five-fingered, three-dimensional smart prosthetic hand.

ACKNOWLEDGMENTS

The financial support for this research from the Telemedicine Advanced Technology Research Center (TATRC) of the U.S. Department of Defense (DoD) is gratefully acknowledged.

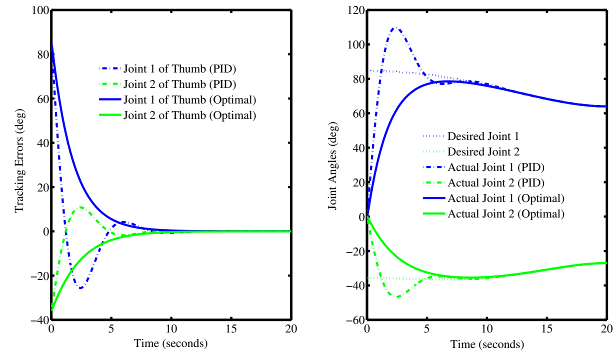

Fig. 6. Tracking Errors (left) and Joint Angles (right) for PID and Optimal Controllers of Thumb

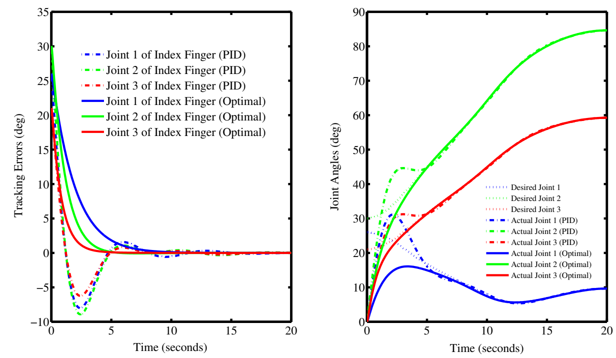

Fig. 7. Tracking Errors (left) and Joint Angles (right) for PID and Optimal Controllers of Index Finger

REFERENCES

[1] M. Zecca, S. Micera, M. Carrozza, and P. Dario, “Control of multifunctional prosthetic hands by processing the electromyographic signal,” *Critical Reviews^{TM} in Biomedical Engineering*, vol. 30, pp. 459–485, 2002, (Review article with 96 references).

[2] J. C. K. Lai, M. P. Schoen, A. Perez-Gracia, D. S. Naidu, and S. W. Leung, “Prosthetic devices: Challenges and implications of robotic implants and biological interfaces,” *Proceedings of the Institute of Mechanical Engineers (IMechE), Part H: Journal of Engineering in Medicine*, vol. 221, no. 2, pp. 173–183, January 2007, special Issue on Micro and Nano Technologies in Medicine.

[3] L. Zollo, S. Roccella, E. Guglielmelli, M. C. Carrozza, and P. Dario, “Biomechatronic design and control of an anthropomorphic artificial hand for prosthetic and robotic applications,” *IEEE/ASME Transactions on Mechatronics*, vol. 12, no. 4, pp. 418–429, August 2007.

[4] D. S. Naidu, C.-H. Chen, A. Perez, and M. P. Schoen, “Control strategies for smart prosthetic hand technology: An overview,” in *Proceedings of the 30th Annual International IEEE EMBS Conference*, Vancouver, Canada, August 20-24 2008, pp. 4314–4317.

[5] D. J. Atkins, D. C. Y. Heard, and W. H. Donovan, “Epidemiologic overview of individuals with upper limb loss and their reported research priorities,” *Journal of Prosthetic and Orthotics*, vol. 8, no. 1, pp. 2–11, 1996.

[6] A. Konar, *Computational Intelligence: Principles, Techniques and Applications*. Berlin, Germany: Springer-Verlag, 2005.

[7] F. Karray and C. De Silva, *Soft Computing and Intelligent Systems Design: Theory, Tools and Applications*. Harlow, England, UK: Pearson Educational Limited, 2004.

[8] Y. Z. Arslan, Y. Hacioglu, and N. Yagiz, “Prosthetic hand finger control using fuzzy sliding modes,” *Journal of Intelligent and Robotic Systems*, vol. 52, pp. 121–138, 2008.

[9] K. Onozato and Y. Maeda, “Learning of inverse-dynamics and inverse-kinematics for two-link scara robot using neural networks,” in *The So-*

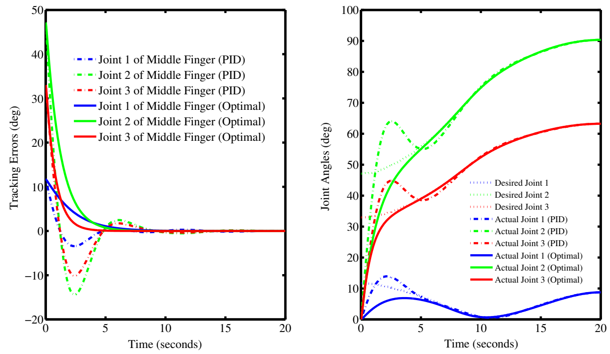

Fig. 8. Tracking Errors (left) and Joint Angles (right) for PID and Optimal Controllers of Middle Finger

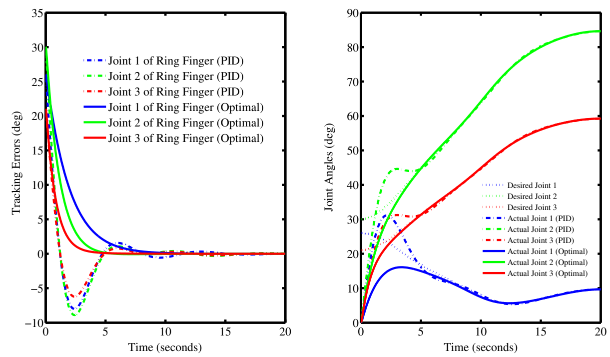

Fig. 9. Tracking Errors (left) and Joint Angles (right) for PID and Optimal Controllers of Ring Finger

ciety of Instrument and Control Engineers (SICE) Annual Conference 2007, Kagawa University, Takamatsu, Japan, September, 17-20 2007, pp. 1031–1034.

[10] V. Aggarwal, G. Singhal, J. He, M. H. Schieber, and N. V. Thakor, "Towards closed-loop decoding of dexterous hand movements using a virtual integration environment," in *30th Annual International IEEE Engineering in Medicine and Biology Society Conference (EMBC 2008)*, Vancouver, British Columbia, Canada, August, 20-24 2008, pp. 1703–1706.

[11] K. K. Tan, S. Huang, and T. H. Lee, "Decentralized adaptive controller design of large-scale uncertain robotic systems," *Automatica*, vol. 45, pp. 161–166, 2009.

[12] R. Kato, H. Yokoi, A. H. Arieta, W. Yub, and T. Arai, "Mutual adaptation among man and machine by using f-mri analysis," *Robotics and Autonomous Systems*, vol. 57, pp. 161–166, 2009.

[13] M. da G. Marcos, J. A. T. Machado, and T.-P. Azevedo-Perdicoulis, "Trajectory planning of redundant manipulators using genetic algorithms," *Communications in Nonlinear Science and Numerical Simulation*, vol. 14, no. 7, pp. 2858–2869, July 2009.

[14] Y. Kamikawa and T. Maeno, "Underactuated five-finger prosthetic hand inspired by grasping force distribution of humans," in *Proceedings of the 2008 IEEE/RSJ International Conference on Intelligent Robots and Systems*, Nice, France, September, 22-26 2008, pp. 717–722.

[15] B. Subudhi and A. S. Morris, "Soft computing methods applied to the control of a flexible robot manipulator," *Applied Soft Computing*, vol. 9, pp. 149–158, 2009.

[16] F. Liu and H. Chen, "Motion control of intelligent underwater robot based on cmac-pid," in *Proceedings of the 2008 IEEE International Conference on Information and Automation*, Zhangjiajie, China, June 20-23 2008.

[17] C.-H. Chen, K. W. Bosworth, M. P. Schoen, S. E. Bearden, D. S. Naidu, and A. Perez, "A study of particle swarm optimization on

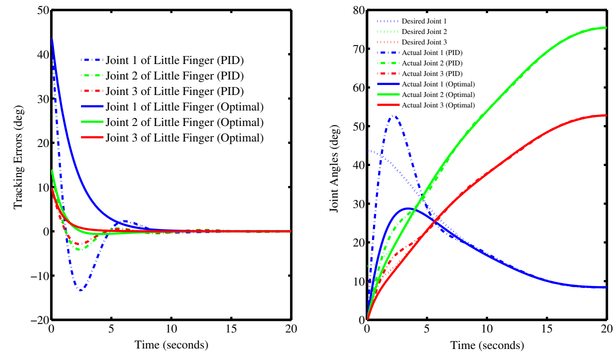

Fig. 10. Tracking Errors (left) and Joint Angles (right) for PID and Optimal Controllers of Little Finger

leukocyte adhesion molecules and control strategies for smart prosthetic hand," in *2008 IEEE Swarm Intelligence Symposium (IEEE SIS08)*, St. Louis, Missouri, USA, September 21-23 2008.

[18] C.-H. Chen, D. S. Naidu, A. Perez, and M. P. Schoen, "Fusion of hard and soft control techniques for prosthetic hand," in *Proceedings of the International Association of Science and Technology for Development (IASTED) International Conference on Intelligent Systems and Control (ISC 2008)*, Orlando, Florida, USA, November 16-18 2008, pp. 120–125.

[19] D. Vrabie, F. Lewis, and M. Abu-Khalaf, "Biologically inspired scheme for continuous-time approximate dynamic programming," *Transactions of the Institute of Measurement and Control*, vol. 30, pp. 207–223, 2008.

[20] D. Naidu, *Optimal Control Systems*. Boca Raton, FL: CRC Press, 2003.

[21] C.-H. Chen, "Hybrid control strategies for smart prosthetic hand," Ph.D. dissertation, Measurement and Control Engineering, Idaho State University, May 2009.

[22] C.-H. Chen, D. S. Naidu, A. Perez-Gracia, and M. P. Schoen, "A hybrid adaptive control strategy for a smart prosthetic hand," in *The 31st Annual International Conference of the IEEE Engineering Medicine and Biology Society (EMBC)*, Minneapolis, Minnesota, USA, September 2-6 2009.

[23] C.-H. Chen, D. Naidu, A. Perez-Gracia, and M. P. Schoen, "A hybrid optimal control strategy for a smart prosthetic hand," in *Proceedings of ASME 2009 Dynamic Systems and Control Conference (DSCC)*, Hollywood, California, USA, October 12-14 2009.

[24] R. R. Seeley, T. D. Stephens, and P. Tate, *Anatomy & Physiology, Eighth Edition*. New York, NY: The McGraw-Hill, 2007.

[25] R. Kelly, V. Santibanez, and A. Loria, *Control of Robot Manipulators in Joint Space*. New York, USA: Springer, 2005.

[26] R. N. Jazar, *Theory of Applied Robotics. Kinematics, Dynamics, and Control*. New York, USA: Springer, 2007.

[27] B. Siciliano, L. Sciavicco, L. Villani, and G. Oriolo, *Robotics: Modelling, Planning and Control*. London, UK: Springer-Verlag, 2009.

[28] F. Lewis, D. Dawson, and C. Abdallah, *Robot Manipulators Control: Second Edition, Revised and Expanded*. New York, NY: Marcel Dekker, Inc.,, 2004.

[29] A. Nikoobin and R. Haghighi, "Lyapunov-based nonlinear disturbance observer for serial n-link robot manipulators," *Journal of Intelligent and Robotic Systems*, 2008, (Published online on 11 December 2008).

[30] M. Marquez, *Nonlinear Control Systems: Analysis and Design*. Hoboken, NJ: Wiley-Interscience, 2003.

[31] P. K. Lavangie and C. C. Norkin, *Joint Structure and Function: A Comprehensive Analysis, Third Edition*. Philadelphia, PA: F. A. Davis Company, 2001.

[32] S. Arimoto, *Control Theory of Multi-fingered Hands: A Modeling and Analytical-Mechanics Approach for Dexterity and Intelligence*. London, UK: Springer-Verlag, 2008.